Contents lists available at ScienceDirect

# Palaeogeography, Palaeoclimatology, Palaeoecology

journal homepage: www.elsevier.com/locate/palaeo

# The earliest Phanerozoic carbonate hardground (Cambrian Stage 5, Series 3): Implications to the paleoseawater chemistry and early adaptation of hardground fauna

Jeong-Hyun Lee [a], Jitao Chen [b], Jusun Woo [c,*]

[a] Department of Earth and Environmental Sciences, Korea University, Seoul 136-713, Republic of Korea
[b] Key Laboratory of Economic Stratigraphy and Palaeogeography, Nanjing Institute of Geology and Palaeontology, Chinese Academy of Sciences, Nanjing 210008, China
[c] Division of Polar Earth-System Sciences, Korea Polar Research Institute, Incheon 406-840, Republic of Korea

## ARTICLE INFO

## ABSTRACT

Carbonate hardgrounds are lithified seafloors formed by synsedimentary cementation of carbonate sediments, which dominantly occur during the period of calcite seas. The earliest typical Phanerozoic hardground known until now was reported from the Furongian of USA, which was suggested to indicate onset of the early Paleozoic calcite sea period. In this study, we report hardgrounds from the early and middle parts of the Cambrian Series 3 (Stage 5 and Drumian) of the North China Platform, which predate previously reported hardgrounds. The hardground surfaces developed on oolitic grainstone, oncolitic wackestone, and microbialite (thrombolite and dendrolite), which sharply truncate the underlying deposits. The radial fibrous calcite cements between the carbonate grains below the hardground surfaces indicate that the cements formed by early marine cementation. EPMA analysis reveals that the fibrous cements typically consist of low-Mg calcite. The hardgrounds are sometimes encrusted by microbialites and coated by hematite, suggesting long exposure to the open seawater after formation of the surface. In addition, detailed review on the sedimentological studies of Cambrian Series 3 to Furongian deposits throughout the world reveals that there may be several other hardgrounds during these times, which could have been overlooked. The abundant occurrence of hardgrounds in Cambrian Series 3 deposits suggests that the general paleoseawater chemistry was suitable to induce synsedimentary cementation of low-Mg calcite, implying that seawater chemistry would have changed from the aragonite to calcite seas during the Cambrian Series 3 or even earlier period. Metazoan encrustors and macroborers possibly could not have adapted to the newly appeared substrate condition yet, until the latest Cambrian Series 3.

© 2015 Elsevier B.V. All rights reserved.

## 1. Introduction

The major seawater chemistry of the oceans oscillated dramatically between aragonite seas (aragonite and high-Mg calcite are dominant precipitant) and calcite seas (low-Mg calcite are dominant precipitant) during the Phanerozoic, which was controlled mainly by changes in Mg/Ca ratio of seawater and temperature (Sandberg, 1983; Hardie, 1996; Balthasar and Cusack, 2015). Although this secular variation in seawater chemistry remains enigmatic, it has been postulated that these changes were influenced by fluctuations in the mid-ocean ridge activity: hot basaltic rocks produced from the mid-ocean ridge removes magnesium from sea water (Hardie, 1996; Müller et al., 2013).

Hardgrounds, synsedimentarily lithified seafloors formed by in situ precipitation of carbonate cement, were widespread during periods of calcite seas (e.g., Ordovician and Jurassic–Cretaceous)

when synsedimentary, inorganic precipitation of calcite was dominant (Wilson and Palmer, 1992; Rozhnov, 2001; Palmer and Wilson, 2004). The occurrence of hardgrounds formed by abiotic precipitation of calcite therefore has been used as an indicator of the calcite seas in the geological record (cf. Zhuravlev and Wood, 2008). The term hardground often includes biological communities consisting of encrusting and boring organisms which encrust the hardground surface (Wilson and Palmer, 1992; Rozhnov, 2001). Strictly speaking, however, hardgrounds can be formed by abiotic cementation of calcite, which does not require biological communities (Wilson and Palmer, 1992). This notion of the abiotic hardground is used throughout this study.

Until now, it has been thought that the earliest Phanerozoic hardground surface ever reported was from the latest part of the Cambrian Series 3 in Iran, but these are formed by microbial activities which enhanced cementation of underlying substrates (Rozhnov, 2001; Kruse and Zhuravlev, 2008). Hardgrounds formed by abiotic cementation of carbonate cements were known to occur from the Furongian, which are encrusted by echinoderms and some spongiomorphs (Brett et al., 1983). During the Ordovician, hardgrounds became abundant in

carbonate successions, which were colonized by various encrustors, macroborers, and cryptic dwellers (Wilson et al., 1992; Taylor and Wilson, 2003).

The occurrence of hardgrounds cemented by low-Mg calcite in the Furongian successions, together with other evidences, such as transition in reef-building organisms, increase in shell bed thickness, and increase of flat-pebble conglomerates, was thought to indicate the beginning of calcite sea period that lasted until the Late Ordovician (cf. Zhuravlev and Wood, 2008; Lee et al., 2015). On the other hand, based on the changes in chemical composition of organisms and fluid inclusions, it has been suggested that calcite seas could have initiated during the late Series 2 to early Series 3 of the Cambrian (Wilson and Palmer, 1992; Wilson et al., 1992; Hough et al., 2006; Porter, 2007, 2010; Zhuravlev and Wood, 2008). The time gap between these two scenarios (ca. 12 Myr) remained problematical.

In this study, we report the occurrence of hardground surfaces from Cambrian Series 3 successions in the eastern North China Platform, which are among the earliest Phanerozoic hardgrounds ever described. The occurrence of hardgrounds in Cambrian Series 3 deposits from the North China Platform and other areas may provide an additional evidence for global changes in seawater chemistry during this time interval. It will also help understand early adaptation history of the hardground communities.

## 2. Geological setting

The North China Platform was a stable epeiric platform during the Cambrian, which was situated near the Indian and Australian margin of Gondwana (Golonka, 2009; McKenzie et al., 2011). According to paleomagnetic analyses, the platform was located near the paleoequator during the Cambrian (Zhao et al., 1992; Huang et al., 2000; Yang et al., 2002). Six lithologic units are identified in the Cambrian succession of Shandong Province, China: the Liguan, Zhushadong, Mantou, Zhangxia, Gushan, and Chaomidian formations, in ascending order (Figs. 1 and 2)

(Chough et al., 2010). The siliciclastic-dominant Liguan and carbonate-dominant Zhushadong formations formed the lowermost units of the Cambrian succession and were deposited during the early Cambrian Series 2 (Stage 3?) (Lee et al., 2014). The Mantou Formation, which mainly consists of fine-grained siliciclastic and minor carbonate sediments, conformably overlies the Zhushadong Formation (Lee and Chough, 2011). Some hardground surfaces are recognized from the carbonate-dominant part of the upper Mantou Formation. Trilobite biozones including *Redlichia chinensis*, *Yaojiayuella*, *Santungaspis*, *Hsuchuangia-Ruichengella*, *Ruichengaspis*, *Sunaspis*, *Poriagraulos*, and *Bailiella* suggest that the formation was deposited during the stages 4 and 5 of the Cambrian (Geyer and Shergold, 2000; Peng et al., 2012). During the late Stage 5–early Guzhangian (*Lioparia*, *Crepicephalina*, *Amphoton-Taitzuia*, and *Damesella-Yabeia* zones), the carbonate-dominant Zhangxia Formation was deposited conformably on the Mantou Formation (Woo et al., 2008), which bears abundant hardgrounds. The Zhangxia carbonate platform was drowned during the late part of Cambrian Series 3, resulting in the shale-dominated Gushan Formation (Chen et al., 2011). After a sea-level fall, carbonate platform was re-established and formed a thick carbonate succession (Chaomidian Formation; Furongian) where hardground surfaces develop on flat-pebble conglomerates and grainstones, as well as microbialites (Lee et al., 2010, 2012; Chen et al., 2011).

## 3. Methods

Ancient hardgrounds are identified based on the existence of features indicating exposure of the cemented seafloor to open seawater. The evidence includes encrusting organisms on hard substrates (e.g., crinoids, bryozoans, and corals), borings (e.g., *Trypanites*), sharp erosional boundaries that truncate underlying substrates, early marine cements, or surfaces coated by iron oxides or phosphate (Brett and Liddell, 1978; Brett and Brookfield, 1984; Wilson and Palmer, 1992; Rozhnov, 2001; Palmer and Wilson, 2004). Due to rare occurrences of
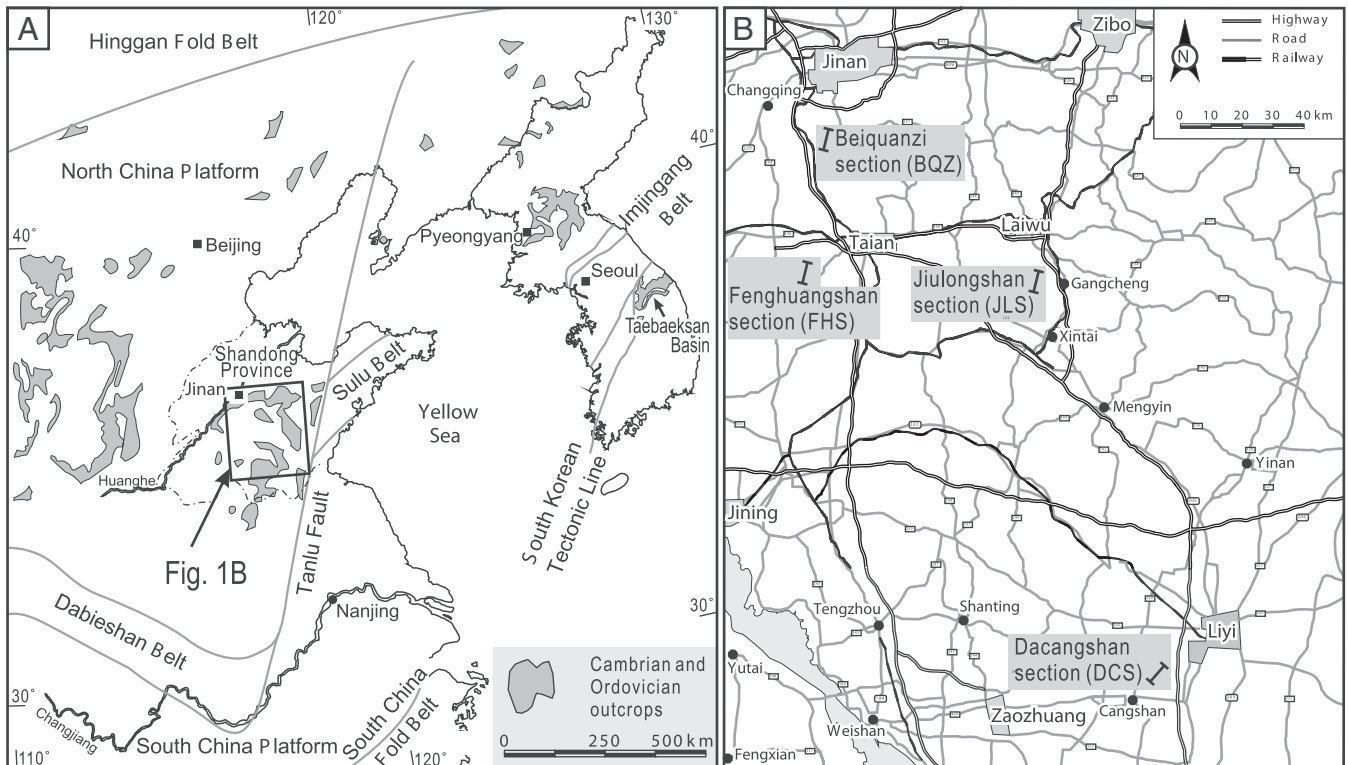


**Fig. 1.** Location map of the study area. BQZ: Beiquanzi section (36°28′47″N, 116°55′30″E), FHS: Fenghuangshan section (36°09′01″N, 116°54′28″E), JLS: Jiulongshan section (36°04′50″N, 117°44′41″E), DCS: Dacangshan section (34°54′14″N, 118°07′03″E).

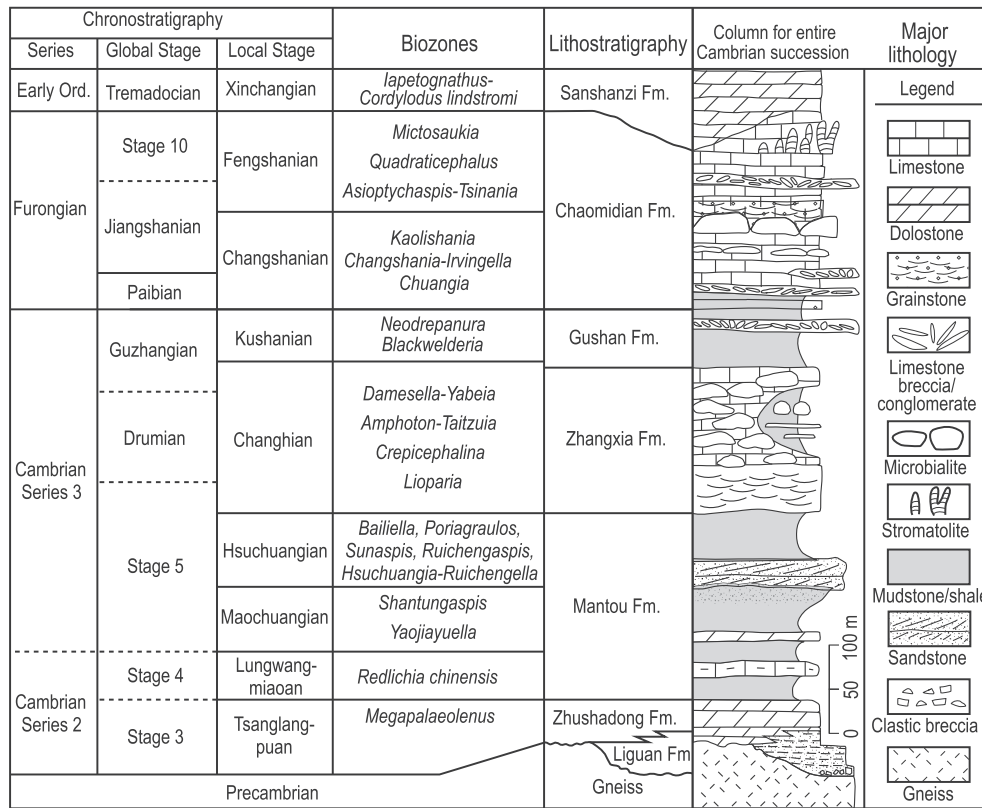| Chronostratigraphy | | | Biozones | Lithostratigraphy | Column for entire Cambrian succession | Major lithology |
|---|---|---|---|---|---|---|
| Series | Global Stage | Local Stage | | | | |
| Early Ord. | Tremadocian | Xinchangian | *Iapetognathus-Cordylodus lindstromi* | Sanshanzi Fm. | | Legend |
| Furongian | Stage 10 | Fengshanian | *Mictosaukia* *Quadraticephalus* *Asioptychaspis-Tsinania* | Chaomidian Fm. | | Limestone |
| | Jiangshanian | Changshanian | *Kaolishania* *Changshania-Irvingella* *Chuangia* | | | Dolostone |
| | Paibian | | | | | Grainstone |
| Cambrian Series 3 | Guzhangian | Kushanian | *Neodrepanura* *Blackwelderia* | Gushan Fm. | | Limestone breccia/ conglomerate |
| | Drumian | Changhian | *Damesella-Yabeia* *Amphoton-Taitzuia* *Crepicephalina* *Lioparia* | Zhangxia Fm. | | Microbialite |
| | Stage 5 | Hsuchuangian | *Bailiella, Poriagraulos, Sunaspis, Ruichengaspis, Hsuchuangia-Ruichengella* | Mantou Fm. | | Stromatolite |
| | | Maochuangian | *Shantungaspis* *Yaojiayuella* | | | Mudstone/shale |
| Cambrian Series 2 | Stage 4 | Lungwang-miaoan | *Redlichia chinensis* | | | Sandstone |
| | Stage 3 | Tsanglang-puan | *Megapalaeolenus* | Zhushadong Fm. Liguan Fm | | Clastic breccia |
| | Precambrian | | | Gneiss | | Gneiss |

**Fig. 2.** Summary of Cambrian stratigraphy of the study area. Modified after Chough et al. (2010).

encrustors and borers in the Cambrian (Wilson and Palmer, 1992; Rozhnov, 2001), it is not easy to identify hardgrounds from Cambrian deposits. We identified hardgrounds in the field based on sharp erosional features, which truncate rigid materials such as carbonate grains (e.g., ooids or oncoids) or microbialite mesostructures (e.g., dendritic clots) below the surface. In addition, we recognized encrusting organisms (microbialites and ?sponges) on hardground surfaces when available.

Detailed observations on the Zhushadong, Mantou, and Zhangxia formations were made to check occurrences of hardgrounds. Hardgrounds are found from the upper part of the Mantou Formation (Stage 5) and the Zhangxia Formation (late Stage 5–Drumian), whereas no hardgrounds were found from the carbonate-dominant Zhushadong Formation (Stage 3?) (Fig. 2). They were described in the field and sampled in order to identify their microscale characteristics. About 50 thin sections were made to understand nature of the hardground surfaces. In order to identify the composition of cements, electron probe microanalysis (EPMA) was carried out on carbon-coated thin sections using a JEOL JXA-8530F electron microprobe. It was operated with four crystal spectrometers (CaO, MgO, FeO, and MnO), and with accelerating voltage of 15 kV and specimen current of 10 nA.

## 4. Hardgrounds in the Cambrian Series 3 of the North China Platform

### 4.1. Description

Three types of hardgrounds are recognized in this study, based on the characteristics of the underlying cemented sediment: oolitic grainstone, oncolitic wackestone, and microbialite (thrombolite or dendrolite). Hardground surfaces developed on top of grainstone/wackestone commonly cut the carbonate grains (e.g., ooids and oncoids) below (Fig. 3). Hardgrounds are most commonly found in thick oolitic grainstone successions (e.g., 32 hardground surfaces within a ca. 6-m-thick succession) and less commonly in microbialites, with minor occurrence in oncolitic

wackestone (Figs. 3–5). The hardground surfaces within oolitic grainstone and oncolitic wackestone can be easily identified in the field based on sharp and relatively flat or undulatory boundaries that truncate grains (Figs. 3A, B, and 4A–C). The surfaces are sometimes coated by hematite (Fig. 4C). These hardgrounds are commonly overlain by grainstone or wackestone, but sometimes by stromatolite (Figs. 3 and 4). In many cases, these hardgrounds are not well traceable; they can be correlated up to a few meters, although some of them can be correlated over a few tens of meters. When hardgrounds develop on the microbialite (thrombolite and dendrolite), the surface flatly cuts underlying microbialite and structures within it (e.g., dendritic microbial clots) (Fig. 5). The hardgrounds developed on the microbialites are commonly overlain by oolites or other microbialites. When hardground surfaces develop within dendrolite, some masses of microbial organisms (dendritic clots) and unknown recrystallized organisms (?sponges) encrust the hardground surfaces (Fig. 5B) (cf. Brett et al., 1983).

In microscale, it is evident that carbonate grains (ooids and oncoids) were truncated by hardground surfaces, although some surfaces experienced secondary stylolitization (Fig. 3C–E). On the other hand, grains above the surface retain their original outlines. Ooids generally retain radial fabric, though some of them are micritized (Fig. 3E). Some angular grains composed of micrites also occur above the surface (Fig. 3D). Some pseudo-hardgrounds also exist within the oolites, characterized by occurrence of calcite spar along the surfaces which cut grains above them (Fig. 3F). The interstitial space between ooids is mainly occluded by radial fibrous cements occurring along the margin of ooids and blocky cements filling the remaining interspace (Fig. 3C–E). Micrite with secondary dolomite rhombs partly fills space between ooids (Fig. 3D). The EPMA analysis reveals that the amount of $MgCO_3$ (mol%) within the fibrous cements from the matrix of oolitic grainstone is generally less than 3% (Table 1). The matrix of the wackestone consists mainly of micrite with some microbial remains such as irregular micritic masses or micritic tubes similar to *Girvanella*. Hematitic coating occurs on some hardground surfaces (Fig. 4C). Some sharply defined
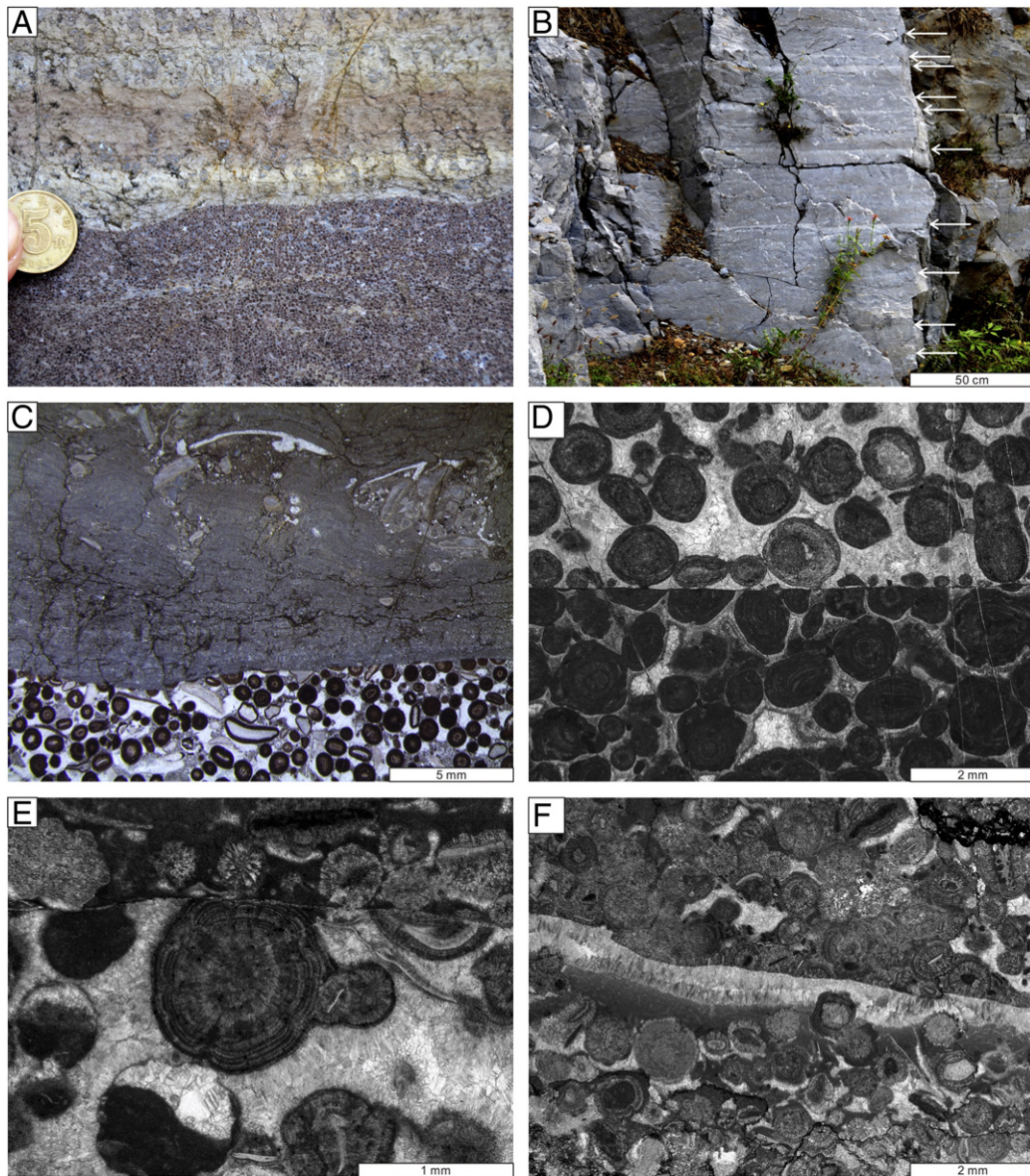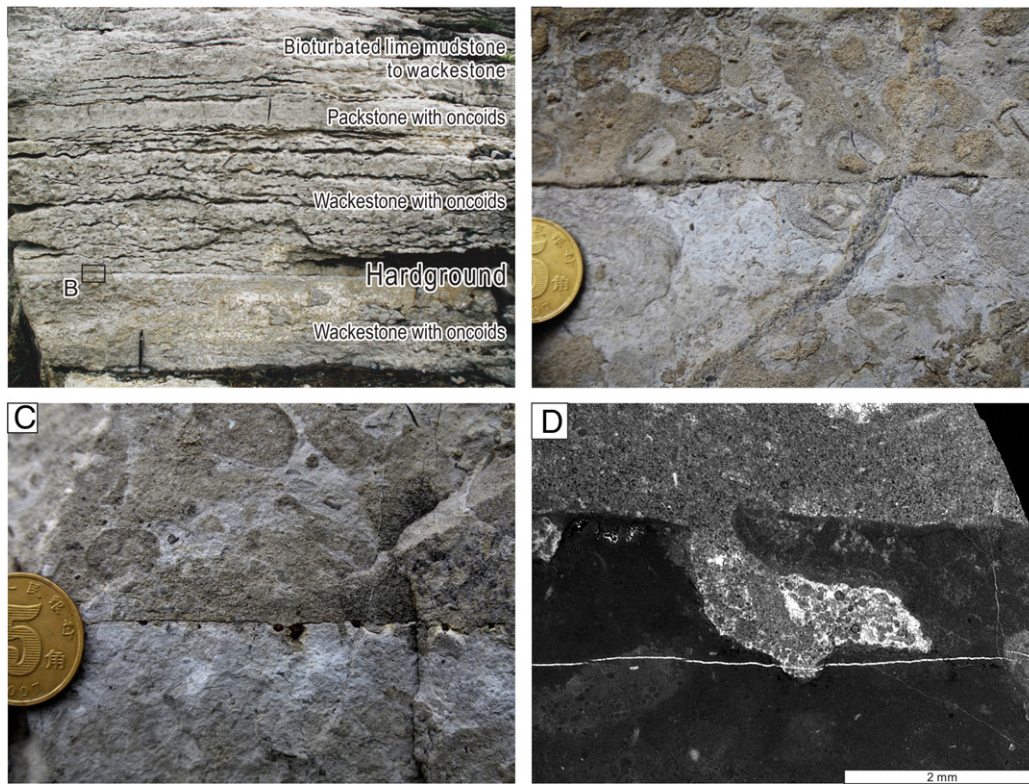
**Fig. 3.** Hardground surfaces developed on the oolitic grainstone (Dacangshan section). For location, see Fig. 1. (A) Photograph of a hardground surface in the Mantou Formation (Cambrian Series 3, Stage 5). Purple ooids are sharply truncated by hardground surface, and overlain by small columnar stromatolite. Coin for scale is 2 cm in diameter. (B) Hardground surfaces (marked by arrows) developed in oolites (Cambrian Series 3, Drumian; Zhangxia Formation). The hardground surfaces are characterized by sharp boundaries and color differences across them. (C) Photomicrograph of a hardground surface from (A). Ooids are sharply cut by the hardground surface and overlain by stromatolite. (D) Photomicrograph of a hardground surface developed within oolite. (E) Radial fibrous cements growing normal to the ooids. Sample is from (B). Some ooids are replaced by micrites and/or sparites. (F) Pseudo-hardground within the oolite. Calcite cements forming this boundary truncate grains above them. Sample is from (B).

bioturbations showing scalloped upper surfaces occur along the surface (Fig. 4D). Due to their small size, it is not possible to fully recognize their three-dimensional structures.

### 4.2. Interpretation

The occurrence of the hardgrounds in successions that deposited in shallow marine environments suggests that they were formed in submarine conditions that experienced early lithification, exposure on the seafloor, and erosion (Marshall and Ashton, 1980; Wilkinson et al., 1982; Chow and James, 1992; Mutti and Bernoulli, 2003). It is most likely that the hardgrounds developed on the top of oolitic grainstone beds were formed by chemical precipitation of carbonates, as there is no evidence of any organism that would have enhanced precipitation (e.g., microbes). On the other hand, subsurface dissolution as a mechanism for formation of the sharp surfaces can be discarded, since the

surfaces only cut the grains below them (Figs. 3–5). Fibrous cements on ooids growing normal to the substrates indicate that these cements formed in situ (Tobin et al., 1996; Palmer and Wilson, 2004). Blocky cements between the ooids would have formed after the fibrous cements during burial. The loose carbonate grains would have been stabilized by precipitation and mutual binding of the grains by fibrous low-Mg calcite cements (<4 mol% $MgCO_3$), forming hardgrounds (Tobin et al., 1996; Palmer and Wilson, 2004; Richter et al., 2011). Dominance of low-Mg calcite within these cements as well as well-preserved radial fabrics of ooids indicate a low Mg/Ca ratio of the seawater from which the cements were precipitated (Stanley and Hardie, 1998, 1999; Palmer and Wilson, 2004). Although the possibility of magnesium loss during burial cannot be fully discarded (e.g., James and Klappa, 1983), very low Mn and Fe concentrations (<400 ppm) in some samples suggest that at least some of the fibrous cements are unaltered or only minimally altered during the diagenesis (Table 1) (Tobin et al., 1996).

**Fig. 4.** Hardground surfaces developed on the oncolitic wackestone (Cambrian Series 3, Drumian; Zhangxia Formation), Beiquanzi section. For location, see Fig. 1. (A) A hardground surface within an oncolitic wackestone facies. Pencil for scale is 14.5 cm in length. (B) A close up view of (A). Note that an oncoid is sharply cut by the hardground surface. Coin for scale in (B) and (C) is 2 cm in diameter. (C) A hardground surface with hematitic coating (arrow) along the surface. (D) Photomicrograph of a hardground surface from (A). Note occurrence of possible boring.

The oolitic hardgrounds, as well as hardgrounds within microbialites, would have developed in high-energy environments such as ooid shoal where ooids were actively formed and deposited (Dravis, 1979, 1983; Chow and James, 1992). Calcites in between ooids would have been precipitated when the ooids were stabilized during periods of low-sedimentation rate (Wilson and Palmer, 1992). Cementation would have initiated slightly below the sediment–water interface, by supersaturated seawater and decreased downward (Shinn, 1969; Dravis, 1979; Wilson and Palmer, 1992; Cornell et al., 2003). Consequently, cemented sediments would have been exposed on the seafloor and truncated by waves and/or currents. On the other hand, the hardgrounds within oncolitic wackestone would have developed in relatively low-energy conditions, which is supported by occurrence of abundant lime mud (Shinn, 1969). In addition, hardgrounds within microbialites and oncolitic wackestone would have been lithified in situ with the aid of microbial mineralization (cf. Dravis, 1979; Hillgärtner et al., 2001). Occurrence of microbialites on the top of hardgrounds together with hematitic coatings suggests that at least some of the hardgrounds were exposed on the seafloor for a long time. Bioturbation in the oncolitic wackestone with scalloped upper surface suggests that the substrate was stiff during their formation. This supports behavioral affinities of the trace-maker to a borer rather than to a burrowing animal. However, a possibility of exhumed burrow that developed on a firmground cannot be fully ruled out.

## 5. Discussion: implications to the global environmental and ecological conditions

In this study, we have shown that hardgrounds occur abundantly within the early to middle parts of Cambrian Series 3 carbonate deposits on the North China Platform. Occurrence of the hardgrounds in Cambrian Stage 5 succession indicates that at least in some localities, seawater chemistry was suitable to induce in situ precipitation of low-Mg calcite.

On the other hand, there are also other reports of Cambrian Series 3 hardgrounds developed within limestone successions (e.g., Chow and James, 1992), many of which were overlooked in previous studies focusing on hardground communities (Fig. 6; Table 2) (cf. Wilson and Palmer, 1992; Rozhnov, 2001; Zhuravlev and Wood, 2008). These Cambrian Series 3 hardgrounds from various localities were characterized by surfaces that flatly truncate the underlying substrates such as lime mudstone, oolitic/oncolitic packstone/grainstone, and limestone conglomerate (Table 2) (e.g., Markello and Read, 1981; Chow and James, 1992; Srinivasan and Walker, 1993). Although most of these hardgrounds (except for one example from the late part of the Cambrian Series 3 in Iran) lack encrusting organisms or borings, similarities between these examples and the present study suggest that these can be real hardgrounds formed by early marine calcite cementation. In addition, there are also some atypical hardgrounds formed by phosphatization in Cambrian Series 3 successions, which are enhanced by characteristic paleoseawater chemistry of this time interval (Fig. 6) (Wilson and Palmer, 1992; Rozhnov, 2001; Creveling et al., 2014). Hardgrounds became generally common during the Furongian, and are sometimes encrusted by echinoderms (Fig. 6; Table 2) (Brett et al., 1983; Sumrall et al., 1997). These hardgrounds mostly developed on top of flat-pebble conglomerates, sharply truncating the underlying substrate. Similar to the Cambrian Series 3 examples, the Furongian hardgrounds most likely formed by calcite precipitation, and were later modified by physical abrasion (Brett et al., 1983).
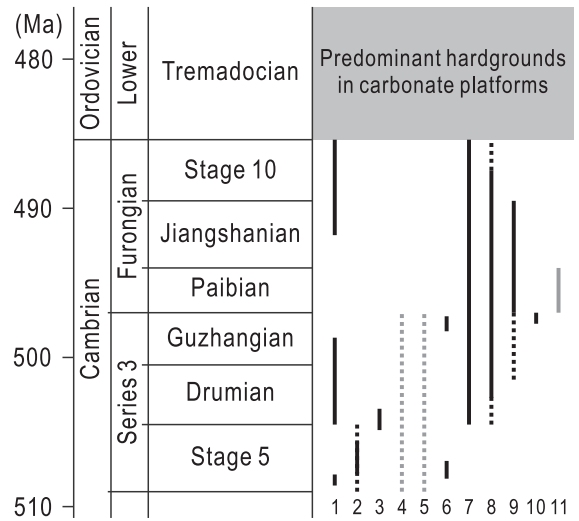
It is noteworthy that the hardground encrusting organisms and macroborers that typically occur in the Ordovician hardgrounds are rare in the Cambrian Series 3 hardgrounds, except for microbialites and ?sponges. On the other hand, firmground-encrusting echinoderms are reported from the Cambrian Stage 5 of western Gondwana (Zamora et al., 2010) and lithistid sponges in the Zhangxia Formation could have encrusted hard substrates within reefs (Lee et al., accepted
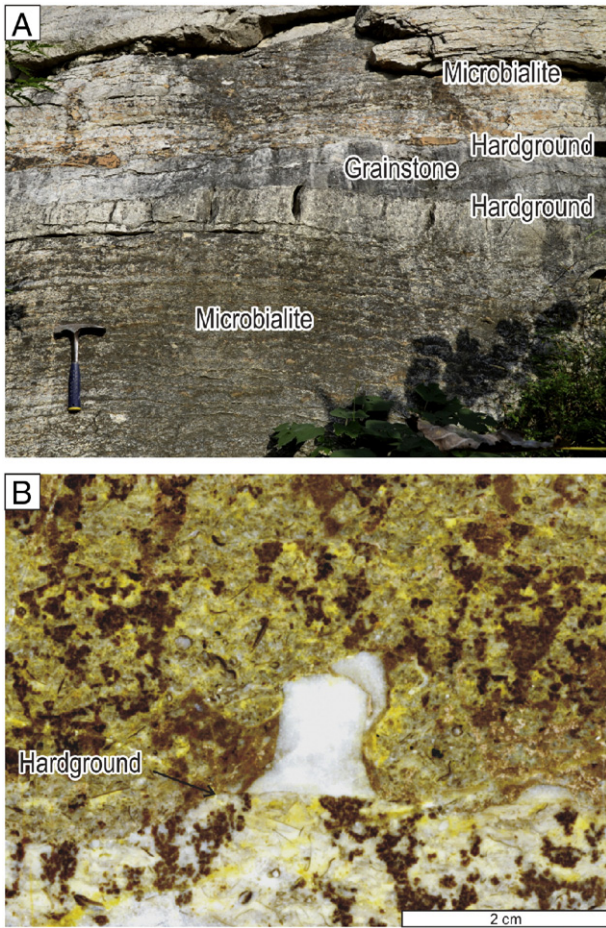
**Fig. 5.** Hardground surfaces developed on microbialites. (A) A hardground developed on top of a microbialite, overlain by bioturbated wackestone (Cambrian Series 3, Drumian; Zhangxia Formation), Beiquanzi Section. Hammer for scale is 28 cm in length. (B) An example of hardground within a dendrolite. The hardground is encrusted by other dendrolite and unidentified calcified organisms (possible sponge) (Cambrian Series 3, Drumian; Zhangxia Formation), Jiulongshan Section. For location, see Fig. 1.



**Fig. 6.** Summary of known hardground surfaces during the Cambrian Series 3 and the Furongian. Black line: carbonate hardgrounds. Grey line: phosphatized hardgrounds. Dotted line: age uncertain. 1: Mantou, Zhangxia, and Chaomidian formations, Shandong Province, China. 2: Bonanza King Formation, Southern Great Basin, USA. 3: Swasey, Wheeler, and Marjum formations, Utah, USA. 4: Aftenstjernesø and Holm Dal formations, Greenland. 5: Thorntonia, Beetle Creek, and Gowers formations, Australia. 6: La Laja Formation (Soldano and Las Torres members), Argentina. 7: March Point, Petit Jardin, and Berry Head formations, Newfoundland, Canada. 8: Maryville, Nolichucky, and Widner Limestone, Elbrook and Conococheague formations, southern Appalachian, USA. 9: Upper Gros Ventre Shale and Snowy Range Formation, Montana/Wyoming, USA. 10: Mila Formation, Iran. 11: Bonneterre Formation, Upper Mississippi Valley, USA. For raw data, see Table 2.

for publication). Absence of metazoan encrustors on the Chinese hardgrounds therefore suggests that these organisms could not have adapted the hardgrounds during the early to middle Cambrian Series 3 yet. The metazoan encrustors such as echinoderms, brachiopods, and lithistid sponges would have advanced to the hardgrounds from the latest Cambrian Series 3 (Kruse and Zhuravlev, 2008) and flourished throughout the Furongian and later periods (Brett et al., 1983; Wilson and Palmer, 1992), together with the macroborers (Taylor and Wilson, 2003; Wilson and Palmer, 2006).

The Cambrian hardgrounds were most likely formed by abiotic mechanisms of rapid calcite cementation (Chow and James, 1992), which is enhanced in calcite seas by the increase in dissolved $CO_2$ in seawater and lowering of the Mg/Ca ratio (Wilson and Palmer, 1992; Wilson et al., 1992; Hardie, 1996; Stanley and Hardie, 1999). Abundant occurrence of hardgrounds in the Cambrian Series 3 deposits of the North China Platform and other previously unrecognized examples collectively suggest that chemical precipitation of carbonate cements was not a local phenomenon; it was a common event during the Cambrian Series 3 and the Furongian in various localities. A significant increase in flat-pebble conglomerates from the Cambrian Series 3 (Zhuravlev and Wood, 2008, and references therein) also supports occurrence of extensive early marine cementation and/or hardground formation during these periods, since formation of flat-pebble requires cementation as well (e.g., Myrow et al., 2004; Chen et al., 2009, and references therein). Abundance of organisms with low-Mg calcite skeletons during the Cambrian Series 3 (Zhuravlev and Wood, 2008) together with an abrupt increase in thickness of average shell beds (Droser and Li, 2001) also suggests a decrease in Mg/Ca ratio of seawater (Stanley and Hardie, 1998, 1999; Porter, 2007, 2010). These data collectively indicate that the transition from aragonite to calcite sea possibly initiated during the Cambrian Stage 5 or even earlier (e.g., Porter, 2007, 2010; Zhuravlev and Wood, 2008; Wood and Zhuravlev, 2012).

**Table 1**
Amount of CaO, MgO, FeO, MnO (wt. %), and MgCO₃ (mol%) within fibrous calcite cements in between ooids. For sample location, see Fig. 1.

| Sample | Location | Age | CaO (wt. %) | MgO (wt. %) | FeO (wt. %) | MnO (wt. %) | MgCO₃ (mol%) |
|---|---|---|---|---|---|---|---|
| DCSMT-1 | DCS (Mantou Fm.) | Cambrian Stage 5 | 55.827 | 0.933 | 0.015 | 0.344 | 2.333 |
| DCSMT-2 | DCS (Mantou Fm.) | Cambrian Stage 5 | 55.875 | 1.433 | 0.021 | 0.030 | 3.583 |
| FHS-1 | FHS (Zhangxia Fm.) | Drumian | 55.273 | 0.548 | 0.025 | 0.014 | 1.370 |
| FHS-2 | FHS (Zhangxia Fm.) | Drumian | 57.589 | 0.253 | 0.105 | 0.020 | 0.633 |
| BQZ-1 | BQZ (Zhangxia Fm.) | Drumian | 50.545 | 0.490 | – | – | 1.225 |
| BQZ-2 | BQZ (Zhangxia Fm.) | Drumian | 57.340 | 0.460 | – | – | 1.150 |

**Table 2**

Summary of the Cambrian Series 3–Furongian hardground surfaces. Phosphatized hardgrounds are marked by grey. Age is corrected based on Peng et al. (2012). Stage names are used when available. References: [1]This study; [2]Osleger and Montañez (1996); [3]Brett et al. (2009); [4]Wilson and Palmer (1992), Ineson and Peel (1997); [5]Southgate (1986), Donnelly et al. (1988); [6]Gomez et al. (2007), Gomez and Astini (2015); [7]Chow and James (1992), Cowan and James (1992, 1993); [8]Markello and Read (1981, 1982), Demicco (1985), Koerschner and Read (1989), Srinivasan and Walker (1993), Rankey et al. (1994); [9]Brett et al. (1983); [10]Kruse and Zhuravlev (2008); [11]Runkel et al. (1998); [12]Brett et al. (1983), Sumrall et al. (1997); [13]Chen et al. (2011), JHL and JC, per. observation.

| Location | Formation | Age | Description |
|---|---|---|---|
| Shandong, China[1] | Mantou and Zhangxia formations | Stage 5–Guzhangian | Hardgrounds sharply truncating underlying oolite, oncolite, and microbialite, partly coated by hematite |
| Southern Great Basin[2] | Bonanza King Formation | Stage 5? | Multiple hardgrounds within peloidal wackestone-packstone |
| Utah[3] | Swasey, Wheeler, and Marjum formations | Stage 5–Drumian | Cemented surfaces with pyritic coatings and corrosion features |
| Greenland[4] | Aftenstjernesø and Holm Dal formations | Cambrian Series 3 | Formed by early diagenetic replacement of cyanobacterial mats by phosphate minerals |
| Australia[5] | Thorntonia, Beetle Creek, and Gowers formations | Cambrian Series 3 | Phosphatic hardgrounds with dark grey-black, phosphate-rich upper rind |
| Argentina[6] | La Laja Formation (Soldano and Las Torres members) | Stage 5 (Soldano Mb.) and Guzhangian (Las Torres Mb.) | Sharp hardground on ribbon limestone/calcarenitic limestones (Soldano Mb.); abundant amalgamated hardgrounds within cross-bedded oolitic grainstone (Las Torres Mb.) |
| Newfoundland[7] | March Point, Petit Jardin, and Berry Head formations | Drumian-Stage 10 | Sub-planar to irregularly undulose surfaces on lime mudstone, skeletal packstone, and oolite; hardgrounds stained and bored; fibrous low-Mg calcite and cement and silty micrite on oolitic hardground |
| Virginia, Tennessee, Maryland (southern Appalachian)[8] | Maryville, Nolichucky, and Widner limestones, Elbrook and Conococheague formations | Drumian-Stage 10 | Hardgrounds truncating underlying lime mudstone, oolitic/oncolitic packstone/grainstone, limestone conglomerate, or quartz silty peloidal packstone, some containing glauconite/pyrite; partly coated with black opaque mineral; some borings |
| Montana/Wyomin[9] | Upper Gros Ventre Shale | Upper Cambrian Series 3 | Truncated upper surfaces on flat pebble conglomerates |
| Iran[10] | Mila Formation | Upper Guzhangian | Hardgrounds formed on shell beds, encrusted by echinoderms |
| Upper Mississippi Valley[11] | Bonneterre Formation | Paibian | Phosphatized and pyritized hardground |
| Montana/Wyoming[12] | Snowy Range Formation | Paibian-Jiangshanian | Slightly hummocky to planar, truncated surfaces of glauconite-rich, carbonate, flat pebble conglomerate, encrusted by echinoderms and microbialites |
| Shandong, China[13] | Chaomidian Formation | Jiangshanian–Stage 10 | Hardgrounds truncating underlying flat pebble conglomerate, grainstone, and microbialite |

## 6. Conclusions

The Cambrian Series 3 deposits of the North China Platform yield abundant carbonate hardgrounds that developed on oolitic grainstone, oncolitic wackestone, and microbialite, and are the earliest Phanerozoic hardgrounds by far. The hardgrounds developed on the grainstone and wackestone were formed by chemical precipitation which cemented and consolidated loose sediment. In addition, there are several other probable examples of hardgrounds in the Cambrian Series 3 deposits previously reported which may have been overlooked. The possible world-wide occurrence of hardgrounds during the Cambrian Series 3 suggests that the seawater chemistry and atmospheric conditions became suitable for the low-Mg carbonate precipitation. Together with an increase in the number of organisms with low-Mg calcite skeletons, the Cambrian Series 3 hardgrounds suggest onset of a calcite sea period that lasted until the Late Ordovician. However, hardground communities including metazoan encrustors and macroborers could not have adapted the newly appeared condition yet; they began to colonize the hardgrounds from the latest Cambrian Series 3 and flourished throughout the Furongian and Ordovician.

## Acknowledgments

## Appendix A. Supplementary data

Supplementary data associated with this article can be found in the online version at http://dx.doi.org/10.1016/j.palaeo.2015.07.043. These data include the Google map of the most important areas described in this article.

## References

Balthasar, U., Cusack, M., 2015. Aragonite-calcite seas—quantifying the gray area. Geology 43, 99–102. http://dx.doi.org/10.1130/g36293.1.

Brett, C.E., Brookfield, M.E., 1984. Morphology, faunas and genesis of Ordovician hardgrounds from southern On tario, Canada. Palaeogeogr. Palaeoclimatol. Palaeoecol. 46, 233–290. http://dx.doi.org/10.1016/0031-0182(84)90001-4.

Brett, C.E., Liddell, W.D., 1978. Preservation and paleoecology of a Middle Ordovician hardground community. Paleobiology 4, 329–348.

Brett, C.E., Liddell, W.D., Derstler, K.L., 1983. Late Cambrian hard substrate communities from Montana/Wyoming: the oldest known hardground encrusters. Lethaia 16, 281–289.

Chen, J., Chough, S.K., Chun, S.S., Han, Z., 2009. Limestone pseudoconglomerates in the Late Cambrian Gushan and Chaomidian Formations (Shandong Province, China): soft-sediment deformation induced by storm-wave loading. Sedimentology 56, 1174–1195. http://dx.doi.org/10.1111/j.1365-3091.2008.01028.x.

Chen, J., Chough, S.K., Han, Z., Lee, J.-H., 2011. An extensive erosion surface of a strongly deformed limestone bed in the Gushan and Chaomidian formations (late Middle Cambrian to Furongian), Shandong Province, China: sequence–stratigraphic implications. Sediment. Geol. 233, 129–149. http://dx.doi.org/10.1016/j.sedgeo.2010.11.002.

Chough, S.K., Lee, H.S., Woo, J., Chen, J., Choi, D.K., Lee, S.-b., Kang, I., Park, T.-y., Han, Z., 2010. Cambrian stratigraphy of the North China Platform: revisiting principal sections in Shandong Province, China. Geosci. J. 14, 235–268. http://dx.doi.org/10.1007/s12303-010-0029-x.

Chow, N., James, N.P., 1992. Synsedimentary diagenesis of Cambrian peritidal carbonates: evidence from hardgrounds and surface paleokarst in the Port au Port Group, Western Newfoundland. Bull. Can. Petrol. Geol. 40, 115–127.

Cornell, S.R., Brett, C.E., Sumrall, C.D., 2003. Paleoecology and taphonomy of an edrioasteroid-dominated hardground association from tentaculitid limestones in

the Early Devonian of New York: a Paleozoic rocky peritidal community. Palaios 18, 212–224. http://dx.doi.org/10.1669/0883-1351(2003)018<0212:PATOAE>2.0.CO;2.

Creveling, J.R., Johnston, D.T., Poulton, S.W., Kotrc, B., Marz, C., Schrag, D.P., Knoll, A.H., 2014. Phosphorus sources for phosphatic Cambrian carbonates. Geol. Soc. Am. Bull. 126, 145–163. http://dx.doi.org/10.1130/b30819.1.

Dravis, J., 1979. Rapid and widespread generation of recent oolitic hardgrounds on a high energy Bahamian Platform, Eleuthera Bank, Bahamas. J. Sediment. Petrol. 49, 195–208. http://dx.doi.org/10.1306/212F76EE-2B24-11D7-8648000102C1865D.

Dravis, J., 1983. Hardened subtidal stromatolites, Bahamas. Science 219, 385–386. http://dx.doi.org/10.1126/science.219.4583.385.

Droser, M.L., Li, X., 2001. The Cambrian radiation and the diversification of sedimentary fabrics. In: Zhuravlev, A.Y., Riding, R. (Eds.), Ecology of the Cambrian Radiation. Columbia University Press, New York, pp. 137–169.

Geyer, G., Shergold, J., 2000. The quest for internationally recognized divisions of Cambrian time. Episodes 23, 188–195.

Golonka, J., 2009. Phanerozoic paleoenvironment and paleolithofacies maps. Early Paleozoic. Geologia 35, 589–654.

Hardie, L.A., 1996. Secular variation in seawater chemistry: An explanation for the coupled secular variation in the mineralogies of marine limestones and potash evaporites over the past 600 m.y. Geology 24, 279–283. http://dx.doi.org/10.1130/0091-7613(1996)024<0279:SVISCA>2.3.CO;2.

Hillgärtner, H., Dupraz, C., Hug, W., 2001. Microbially induced cementation of carbonate sands: are micritic meniscus cements good indicators of vadose diagenesis? Sedimentology 48, 117–131. http://dx.doi.org/10.1046/j.1365-3091.2001.00356.x.

Hough, M.L., Shields, G.A., Evins, L.Z., Strauss, H., Henderson, R.A., Mackenzie, S., 2006. A major sulphur isotope event at c. 510 Ma: a possible anoxia–extinction–volcanism connection during the Early–Middle Cambrian transition? Terra Nova 18, 257–263. http://dx.doi.org/10.1111/j.1365-3121.2006.00687.x.

Huang, B., Zhu, R., Otofuji, Y.-i., Yang, Z., 2000. The Early Paleozoic paleogeography of the North China block and the other major blocks of China. Chin. Sci. Bull. 45, 1057–1065. http://dx.doi.org/10.1007/BF02887174.

James, N.P., Klappa, C.F., 1983. Petrogenesis of Early Cambrian reef limestones, Labrador, Canada. J. Sediment. Petrol. 53, 1051–1096. http://dx.doi.org/10.1306/212F831E-2B24-11D7-8648000102C1865D.

Kruse, P.D., Zhuravlev, A.Y., 2008. Middle-Late Cambrian Rankenella-Girvanella reefs of the Mila Formation, northern Iran. Can. J. Earth Sci. 45, 619–639. http://dx.doi.org/10.1139/e08-016.

Lee, H.S., Chough, S.K., 2011. Depositional processes of the Zhushadong and Mantou formations (Early to Middle Cambrian), Shandong Province, China: roles of archipelago and mixed carbonate–siliciclastic sedimentation on cycle genesis during initial flooding of the North China Platform. Sedimentology 58, 1530–1572. http://dx.doi.org/10.1111/j.1365-3091.2011.01225.x.

Lee, J.-H., Chen, J., Chough, S.K., 2010. Paleoenvironmental implications of an extensive maceriate microbialite bed in the Furongian Chaomidian Formation, Shandong Province, China. Palaeogeogr. Palaeoclimatol. Palaeoecol. 297, 621–632. http://dx.doi.org/10.1016/j.palaeo.2010.09.012.

Lee, J.-H., Chen, J., Chough, S.K., 2012. Demise of an extensive biostromal microbialite in the Furongian (late Cambrian) Chaomidian Formation, Shandong Province, China. Geosci. J. 16, 275–287. http://dx.doi.org/10.1007/s12303-012-0027-2.

Lee, J.-H., Lee, H.S., Chen, J., Woo, J., Chough, S.K., 2014. Calcified microbial reefs in the Cambrian Series 2 of the North China Platform: implications for the evolution of Cambrian calcified microbes. Palaeogeogr. Palaeoclimatol. Palaeoecol. 403, 30–42. http://dx.doi.org/10.1016/j.palaeo.2014.03.020.

Lee, J.-H., Chen, J., Chough, S.K., 2015. The middle–late Cambrian reef transition and related geological events: a review and new view. Earth Sci. Rev. 145, 66–84. http://dx.doi.org/10.1016/j.earscirev.2015.03.002.

Lee, J.-H., Woo, J., Lee, D.-J., 2015. The earliest reef-building anthaspidellid sponge Rankenella zhangxianensis n. sp. from the Zhangxia Formation (Cambrian Series 3), Shandong Province, China. J. Paleontol. (accepted for publication).

Markello, J.R., Read, J.F., 1981. Carbonate ramp-to-deeper shale shelf transitions of an Upper Cambrian intrashelf basin, Nolichucky Formation, Southwest Virginia Appalachians. Sedimentology 28, 573–597. http://dx.doi.org/10.1111/j.1365-3091.1981.tb01702.x.

Marshall, J.D., Ashton, M., 1980. Isotopic and trace element evidence for submarine lithification of hardgrounds in the Jurassic of eastern England. Sedimentology 27, 271–289. http://dx.doi.org/10.1111/j.1365-3091.1980.tb01178.x.

McKenzie, N.R., Hughes, N.C., Myrow, P.M., Choi, D.K., Park, T.-y., 2011. Trilobites and zircons link north China with the eastern Himalaya during the Cambrian. Geology 39, 591–594. http://dx.doi.org/10.1130/g31838.1.

Müller, R.D., Dutkiewicz, A., Seton, M., Gaina, C., 2013. Seawater chemistry driven by supercontinent assembly, breakup, and dispersal. Geology 41, 907–910. http://dx.doi.org/10.1130/g34405.1.

Mutti, M., Bernoulli, D., 2003. Early marine lithification and hardground development on a Miocene ramp (Maiella, Italy): key surfaces to track changes in trophic resources in nontropical carbonate settings. J. Sediment. Res. 73, 296–308. http://dx.doi.org/10.1306/083102730296.

Myrow, P.M., Tice, L., Archuleta, B., Clark, B., Taylor, J.F., Ripperdan, R.L., 2004. Flat-pebble conglomerate: its multiple origins and relationship to metre-scale depositional cycles. Sedimentology 51, 973–996. http://dx.doi.org/10.1111/j.1365-3091.2004.00657.x.

Palmer, T., Wilson, M., 2004. Calcite precipitation and dissolution of biogenic aragonite in shallow Ordovician calcite seas. Lethaia 37, 417–427. http://dx.doi.org/10.1080/00241160410002135.

Peng, S., Babcock, L.E., Cooper, R.A., 2012. The Cambrian Period. In: Gradstein, F.M., Ogg, J.G., Schmitz, M., Ogg, G. (Eds.), The Geologic Time Scale 2012. Elsevier, pp. 437–488 http://dx.doi.org/10.1016/b978-0-444-59425-9.00019-6.

Porter, S.M., 2007. Seawater chemistry and early carbonate biomineralization. Science 316, 1302. http://dx.doi.org/10.1126/science.1137284.

Porter, S.M., 2010. Calcite and aragonite seas and the de novo acquisition of carbonate skeletons. Geobiology 8, 256–277. http://dx.doi.org/10.1111/j.1472-4669.2010.00246.x.

Richter, D.K., Neuser, R.D., Schreuer, J., Gies, H., Immenhauser, A., 2011. Radiaxial-fibrous calcites: a new look at an old problem. Sediment. Geol. 239, 23–36. http://dx.doi.org/10.1016/j.sedgeo.2011.06.003.

Rozhnov, S.V., 2001. Evolution of the hardground community. In: Zhuravlev, A.Y., Riding, R. (Eds.), Ecology of the Cambrian Radiation. Columbia University Press, New York, pp. 238–253.

Sandberg, P.A., 1983. An oscillating trend in Phanerozoic non-skeletal carbonate mineralogy. Nature 305, 19–22. http://dx.doi.org/10.1038/305019a0.

Shinn, E.A., 1969. Submarine lithification of Holocene carbonate sediments in the Persian Gulf. Sedimentology 12, 109–144. http://dx.doi.org/10.1111/j.1365-3091.1969.tb00166.x.

Srinivasan, K., Walker, K.R., 1993. Sequence stratigraphy of an intrashelf basin carbonate ramp to rimmed platform transition: Maryville Limestone (Middle Cambrian), southern Appalachians. Geol. Soc. Am. Bull. 105, 883–896. http://dx.doi.org/10.1130/0016-7606(1993)105<0883:ssoaib>2.3.co;2.

Stanley, S.M., Hardie, L.A., 1998. Secular oscillations in the carbonate mineralogy of reef-building and sediment-producing organisms driven by tectonically forced shifts in seawater chemistry. Palaeogeogr. Palaeoclimatol. Palaeoecol. 144, 3–19. http://dx.doi.org/10.1016/S0031-0182(98)00109-6.

Stanley, S.M., Hardie, L.A., 1999. Hypercalcification: paleontology links plate tectonics and geochemistry to sedimentology. GSA Today 9, 1–7.

Sumrall, C.D., Sprinkle, J., Guensburg, T.E., 1997. Systematics and paleoecology of Late Cambrian echinoderms from the Western United States. J. Paleontol. 71, 1091–1109.

Taylor, P.D., Wilson, M.A., 2003. Palaeoecology and evolution of marine hard substrate communities. Earth Sci. Rev. 62, 1–103. http://dx.doi.org/10.1016/s0012-8252(02)00131-9.

Tobin, K.J., Walker, K.R., Steinhauff, D.M., Mora, C.I., 1996. Fibrous calcite from the Ordovician of Tennessee: preservation of marine oxygen isotopic composition and its implications. Sedimentology 43, 235–251. http://dx.doi.org/10.1046/j.1365-3091.1996.d01-2.x.

Wilkinson, B.H., Janecke, S.U., Brett, C.E., 1982. Low-magnesian calcite marine cement in Middle Ordovician hardgrounds from Kirkfield, Ontario. J. Sediment. Petrol. 52, 47–57. http://dx.doi.org/10.1306/212F7ED7-2B24-11D7-8648000102C1865D.

Wilson, M.A., Palmer, T.J., 1992. Hardground and hardground faunas. Institute of Earth Studies Publication 9. University of Wales, Aberystwyth (131 pp.).

Wilson, M.A., Palmer, T.J., 2006. Patterns and processes in the Ordovician bioerosion revolution. Ichnos 13, 109–112. http://dx.doi.org/10.1080/10420940600850505.

Wilson, M.A., Palmer, T.J., Guensburg, T.E., Finton, C.D., Kaufman, L.E., 1992. The development of an Early Ordovician hardground community in response to rapid sea-floor calcite precipitation. Lethaia 25, 19–34. http://dx.doi.org/10.1111/j.1502-3931.1992.tb01789.x.

Woo, J., Chough, S.K., Han, Z., 2008. Chambers of Epiphyton thalli in microbial buildups, Zhangxia Formation (Middle Cambrian), Shandong Province, China. Palaios 23, 55–64. http://dx.doi.org/10.2110/palo.2006.p06-103r.

Wood, R., Zhuravlev, A.Y., 2012. Escalation and ecological selectively of mineralogy in the Cambrian Radiation of skeletons. Earth Sci. Rev. 115, 249–261. http://dx.doi.org/10.1016/j.earscirev.2012.10.002.

Yang, Z., Otofuji, Y.-i., Sun, Z., Huang, B., 2002. Magnetostratigraphic constraints on the Gondwanan origin of North China: Cambrian/Ordovician boundary results. Geophys. J. Int. 151, 1–10. http://dx.doi.org/10.1046/j.1365-246X.2002.01656.x.

Zamora, S., Clausen, S., Alvaro, J.J., Smith, A.B., 2010. Pelmatozoan echinoderms as colonizers of carbonate firmgrounds in mid-Cambrian high energy environments. Palaios 25, 764–768. http://dx.doi.org/10.2110/palo.2010.p10-052r.

Zhao, X., Coe, R.S., Liu, C., Zhou, Y., 1992. New Cambrian and Ordovician paleomagnetic poles for the North China Block and their paleogeographic implications. J. Geophys. Res. 97, 1767–1788. http://dx.doi.org/10.1029/91JB02742.

Zhuravlev, A.Y., Wood, R.A., 2008. Eve of biomineralization: controls on skeletal mineralogy. Geology 36, 923–926. http://dx.doi.org/10.1130/g25094a.1.